SERS nanotags for Folate Receptor α detection at the single cell level: discrimination of overexpressing cells and potential for live cell applications

Alexandre Verdin[1], Sian Sloan-Dennison[2], Cedric Malherbe[1], Duncan Graham[2] and Gauthier Eppe[1].

[1]*Mass Spectrometry Laboratory, MolSys Research Unit, University of Liège, Allée du 6 Août, 4000 Liège, Belgium.*

[2]*Department of Pure and Applied Chemistry, Technology and Innovation Center, University of Strathclyde, 99 George Street, Glasgow G1 1RD, UK.*

Abstract

Folate Receptor α (FRα) is a high affinity folate membrane receptor that is overexpressed in a wide variety of cancers. Detecting the overexpression of this receptor is important for cancer cells identification and to potentially guide the choice of treatment since several FRα-targeted drugs are currently in clinical trials. In this work, we built SERS nanotags based on core@shell Au@Ag nanoparticles labelled with resonant Raman-reporter and functionalised with a thiolated PEG linker bearing folic acid at the chain end. Using SERS mapping on single cells, we showed that the nanotags (FR-nanotags) could specifically target FRα on overexpressing HeLa cells and could measure the gradual blocking of FRα by free folic acid introduced in the media along the nanotags. With a control nanotag, we showed that the SERS response was 10-fold higher on HeLa cells when folic acid is present on the PEG linker compared to PEG chains without folic acid. Non-specific binding of the FR-nanotags was demonstrated to be low and mainly caused by the folic acid molecule at the PEG chain end. When comparing cancer cells with different expression level of FRα, we obtained 4-fold higher SERS response on overexpressing HeLa cells compared to non-overexpressing A549 cells, allowing the discrimination of both cell lines with a high contrast. Owing to the biocompatibility of the developed nanotags, we demonstrated that measurements of FRα on live HeLa cells were also possible and gave similar results than measurements on fixed cells, indicating the versatility of the developed nanotags for detecting FRα in various experimental conditions.

Introduction

In oncology, the need to quantify specific molecular targets related to tumors has been continuously growing and the development of assays capable of measuring the potential overexpression of membrane proteins directly on cancerous cells is a highly active research area [1], [2]. Indeed, the overexpression of some membrane proteins can be used to target specifically cancerous cells with drugs bearing protein-specific targeting moieties such as antibodies, aptamers or small molecules [3]–[6]. The overexpression of membrane proteins can also give insight on the evolution of the tumor and is of significant importance for prognosis [7]. Folate Receptor α (FRα) is a membrane receptor responsible for the uptake of folic acid, a vitamin necessary for DNA synthesis [8]. Therefore, this receptor is overexpressed by a wide variety of cancerous cells and allows higher uptake of folic acid that enables the cells to grow and multiply faster than healthy cells [9]. FRα is a relatively new candidate for specific drug targeting, notably in the case of lung and ovarian cancer since those cancers generally exhibit a high overexpression of FRα [8]. There are currently about 10 clinical trials aiming at developing FRα-targeted drugs for cancer treatment [10]. It is widely accepted that to optimally select the patient most likely to benefit from those treatments, the expression of FRα must be assessed with the highest possible accuracy. FRα offers the advantage of highly specific targeting with a stable, cheap and chemically-modifiable molecule, folic acid, circumventing the use of antibodies. Indeed, folic acid exhibits a high affinity for FRα ($K_d \approx 0.1 – 1$ nM) [11] and a lower affinity for other types of folate transporters (μM

This is a peer-reviewed, accepted author manuscript of the following article: Verdin, A., Sloan-Dennison, S., Malherbe, C., Graham, D., & Eppe, G. (2022). SERS nanotags for folate receptor α detection at the single cell level: discrimination of overexpressing cells and potential for live cell applications. Analyst. https://doi.org/10.1039/D2AN00706A

range) [12], and several studies have shown that chemical modifications of the γ-carboxylic function of this molecule does not lead to a significant loss of targeting ability [13], [14]. Previously reported optical methods to detect FRα on single cells mainly relies on fluorescence [15], [16], which suffers from limitations due to the photobleaching of the fluorescent molecules and due to interferences from the autofluorescence of cells. Alternative analytical methods are therefore needed to circumvent the current limitations.

Surface-Enhanced Raman Spectroscopy (SERS) is a highly sensitive technique that holds great promises for the bio-analytical field [17]. During the last decade, many groups have put huge efforts into translating SERS from research laboratories to real-world applications [18]–[20]. Notably, nanotags based on SERS-active nanoparticles have been continuously improved in terms of brightness, stability and reproducibility since they offer an ideal alternative to fluorescent labels for specific indirect detection of biological targets [21]–[23]. SERS nanotags have several advantages over techniques such as fluorescence or immunohistochemistry (IHC) for measurement of biological samples. Notably, SERS nanotags are resistant to photobleaching and their spectral signature is easily distinguishable from cell and tissue autofluorescence [24]. Moreover, the plasmonic nanosubstrate can be engineered to provide very high signal enhancement, eliminating the need for an amplification step that is usually necessary for fluorescence and IHC measurements [25]–[27]. Finally, SERS nanotags allow higher multiplexing capabilities owing to their narrow spectral features [28], [29]. Such nanotags have already been used to detect a wide variety of membrane proteins. For example, nanotags targeted at the Human Epidermal Growth Factor Receptor 2 (HER-2) allow evaluation of its overexpression in single cells as well as on tissue sections [25], [30]–[32]. Epidermal Growth Factor Receptor (EGFR) [33], [34] is also a popular target, and other examples have been provided by various groups by targeting PDL1 [35], [36], EpCAM [26], CD44 [37] and others [38]. Recently, Faulds *et al.* showed that SERS nanotags could be used to measure the expression of Estrogen Receptor α (ERα), and could also be used to measure the effect of an ERα-disrupting drug directly on ERα-overexpressing breast cancer cells and spheroids [39], [40]. Xu *et al*. demonstrated that SERS nanotags that targeted N-cadherin could monitor the effect of metformin hydrochloride on breast cancer cells [41]. Those recent advances emphasize the need to provide SERS nanotags capable of measuring membrane markers at the cellular level with the aim of guiding the choice of treatment in the future.

Therefore, we propose to apply SERS nanotags functionalised with folic acid for the specific detection and quantification of FRα on cancerous cells. Previous works reporting SERS nanotags targeting FRα mainly focus on location while quantitative information is needed for applications [42]–[45]. Moreover, limitations caused by the design of the nanotags have occurred, notably due to (i) the use of non-resonant Raman reporters, inherently limiting the sensitivity [42], [46], [47], (ii) the absence of a protective coating on the surface of the nanotags, potentially causing spectral interferences during SERS measurements [44], [46], [48] and (iii) the use of cationic polymer coatings, which are not ideal to prevent non-specific interactions on the negatively-charged cellular membrane [43], [49], [50].

In this work, we used core@shell gold@silver nanoparticles (Au@Ag NPs) as the Raman-enhancing substrate owing to their high enhancement and multi-wavelength excitation capabilities [25], [49]. Those NPs were combined with malachite green isothiocyanate (MGITC) to further profit from the resonance Raman enhancement of this molecule under red laser irradiation, allowing us to reach even higher sensitivity through surface-enhanced resonance Raman scattering (SERRS) [51]. The specificity toward FRα was provided by a thiolated PEG linker functionalised with folic acid. This PEG coating simultaneously provided the targeting effect, limited non-specific interactions and allowed the efficient stabilisation of the SERS nanotag in complex biological media. The nanotags produced were thoroughly characterised by various physico-chemical techniques to further understand their structure and stability.

Using SERS imaging of single cells, we showed that the developed nanotags (denoted FR-nanotags) specifically target FRα by performing various blocking and control experiments on FRα-overexpressing

HeLa cells. We also studied non-specific interactions on HeLa cells using a control nanotag bearing no folic acid at the PEG chain end, illustrating that folic acid is also responsible for some part of the non-specific interactions on cells. Then, we demonstrated that the nanotags can efficiently discriminate between FRα-overexpressing (HeLa) and non-overexpressing (A549) cancerous cells. We obtained a 4-fold higher SERS response in HeLa cells compared to A549 cells. This high contrast between both kinds of cells constitutes a major improvement compared to our previous work using a cationic polymer coating (poly(allylamine)) on the nanotags [49]. Finally, we showed that the nanotags exhibited minimal cellular toxicity, allowing us to use the tags in live cell imaging experiments. We demonstrated that the nanotags were also able to monitor the status of FRα on live HeLa cells, with results similar to those obtained on fixed cells. The results indicate that the chemical fixation step or the drying of the cells did not lead to a significant change in the detection of the SERS nanotags, which indicates the high versatility of the nanotags and their broader applicability for FRα detection.

Material and Methods

Chemicals

Gold nanoparticles of 40 nm were purchased from NanoQ (Belgium) at an optical density of 4 at 529 nm ($2.5x10^{11}$ NPs/mL). Silver nitrate and ascorbic acid were purchased from Sigma Aldrich. Thiol-poly(ethylene)glycol-folic acid (HS-PEG-FA) with an average molecular weight of 5000 g/mol was purchased from Abbexa. Malachite Green isothiocyanate was purchased from Thermo Fischer.

Instrumentation

UV-Visible extinction spectra were measured with an Agilent Cary 60 spectrophotometer. Nanoparticles were diluted to $2.5x10^{10}$ NPs/mL in MilliQ water and spectra were measured through a PMMA disposable cuvette in the range of 330 to 800 nm. Zeta potential and dynamic light scattering (DLS) measurements were obtained with a Malvern Nanosizer Nano ZS and the NPs concentration was also of $2.5x10^{10}$ NPs/mL. Negatively-charged 40 nm polystyrene beads were measured as reference material before running the samples. SERS measurements in solution were carried on a Snowy Range handheld Raman spectrometer with a wavelength of 638 nm. 500 µL of NPs at a concentration of $2.5x10^{11}$ NPs/mL were placed in glass vials for measurements. Spectra were acquired with an approximate power at the sample of 1 mW and with 3 acquisitions of 1 s. Spectra were then exported as .spc files and baseline-corrected in Labspec software (Horiba) using a polynomial fit. SERS mapping experiments were carried out on an InVia Renishaw microscope.

Nanotags synthesis

Au@Ag NPs were synthesised according to our previously reported method [49]. Au@Ag NPs ($2.5x10^{11}$ NP/mL) were render SERS-active by adding 50 µL of MGITC 10^{-5} M to 500 µL of Au@Ag NPs and incubated on a shaking plate for 30 min (final concentration of $9.1x10^{-7}$ M). Then, 20 µL of HS-PEG-FA $5x10^{-5}$ M were added to the SERS-activated Au@Ag NPs and incubated on a shaking plate for 2 hours (final concentration of $1.75x10^{-6}$ M). The resulting SERS nanotags were centrifuged at 5000 RPM for 15 min and resuspended in MilliQ water to their initial concentration. Nanotags were kept at 4°C until further use.

Cell culture

A549 cells were purchased from the European Collection of Authenticated Cell cultures (ECACC). HeLa and A549 cells were cultured in DMEM media supplemented with 10% FBS, 1% streptomycin/penicillin and 1% fungizone. 100 000 cells were seeded on sterile glass cover slips and incubated with complete media for 24 h at 37°C and under 5% CO_2 atmosphere to allow cells to adhere to the glass slide. For SERS experiments, media was removed and cells were incubated for 4 hours at 37°C and under 5% CO_2 atmosphere with fresh media containing the nanotags (40 pM). For specificity

study on HeLa cells, media containing the nanotags (40 pM) and folic acid (50 or 100 µM) was incubated with the cells for 4 hours. Control experiments with the non-targeted nanotags were conducted similarly. A549 cells were grown with the same media and in the same conditions. Incubation of the nanotags on A549 cells was carried on similarly as the HeLa cells (40 pM, 4 hours). After incubation with the nanotags, cells were rinsed 3 times with phosphate buffer saline solution (PBS), fixed 15 min with 4% formaldehyde in PBS at room temperature, and washed a last time with PBS before drying and SERS mapping. For live cells measurements, cells were placed in PBS at 37°C after the incubation period with the nanotags and directly mapped using a water immersion objective.

Raman measurements

The binding of FR-nanotags was measured using Raman mapping. Maps were obtained with a Renishaw InVia confocal Raman spectrometer. For fixed cells, a 50x objective (NA = 0.75) was used to map the cells with a spatial resolution of 1 µm in both x and y directions. The 633 nm excitation from a He-Ne laser was used with an approximate power at the sample of 8 mW. Spectra were measured with a single acquisition of 1 s per point, and using a 1200 L mm^{-1} grating. For live cells, a 60x water immersion objective (NA = 1.0) was used with a single acquisition of 0.5 s and 4 mW power at the sample. Other parameters for mapping remained similar to the fixed cells experiments. WiRe 4.2 (Renishaw) software was used for data pre-processing. Spectra were baseline corrected and cosmic rays were removed. The SERS images were generated by using the direct classical least square (DCLS) function with the reference spectrum of MGITC. This function provides a fitting score between 0 and 1, with values close to 1 characterising experimental spectrum that fits well with the reference spectrum of MGITC. Only spectra with a fitting score > 0.4 [39] were retained for further analysis, and pixels corresponding to these spectra were displayed and overlaid to the optical image of the cells. At least 5 cells were fully mapped in every experimental condition.

SERS maps processing

SERS maps were processed according to the paper of Kapara *et al.* [39]. Briefly, after DCLS analysis of the SERS maps, only the pixels with fit coefficient > 0.4 were kept. All the pixels satisfying this criterion were set to the same color intensity (monochromatic red color scale). Then, images were exported in ImageJ software. The area of the cell in terms of pixels was first measured. Then, the red pixels (corresponding to pixels with SERS signal of MGITC) were extracted by thresholding and their area were also measured using the particle analysis function. Finally, we computed the ratio between the area of SERS-active pixels and the total area of the cell. The metric obtained is defined as the percentage of SERS-responsive pixels. Average SERS spectra were constructed for some representative cells in several experimental conditions by averaging all the SERS spectra highlighted by the DCLS analysis for a particular cell.

Results and Discussion

Nanotags characterisation

Nanotags designed to target FRα on cancer cells were characterised by various physico-chemical techniques to assess their functionalisation and stability. A schematic representation of the developed nanotags is presented in **Figure 1** and their characterisation is shown in **Figure 2**. As observed by UV-Vis spectroscopy, bare Au@Ag NPs have a localised surface plasmon resonance (LSPR) located at 395 nm and a slight shouldering around 490 nm due to the contribution of the gold core (**Figure 2A**). These optical properties allow them to be used efficiently at various excitation wavelengths as we demonstrated in previous works [25], [49]. After functionalisation with the Raman-reporter MGITC, the position of the maximum of extinction does not shift significantly (**Figure 2A**). Moreover, the extinction at high wavelength (> 600 nm) also does not increase significantly, indicating the absence of aggregation of the NPs upon functionalisation. The concentration of MGITC was carefully optimised in our synthesis protocol in order to reach the highest possible SERS signal without causing significant

destabilisation of the NPs (**Figure S1**). The targeting ability toward FRα was introduced through a thiolated PEG linker functionalised with folic acid at the end of the chain (denoted HS-PEG-FA). The presence of folic acid at the end of the chain was confirmed by UV-Vis and infrared spectroscopies (**Figure S2**). Upon functionalisation with HS-PEG-FA, the position of the LSPR shifted from 395 to 399 nm (**Figure 2A**). This red shift was caused by a change of the refractive index at the surface of the NPs due to the presence of PEG. We also observed a broadening of the extinction band upon functionalisation with the PEG linker which further confirms the presence of the polymer on the surface of the NPs.

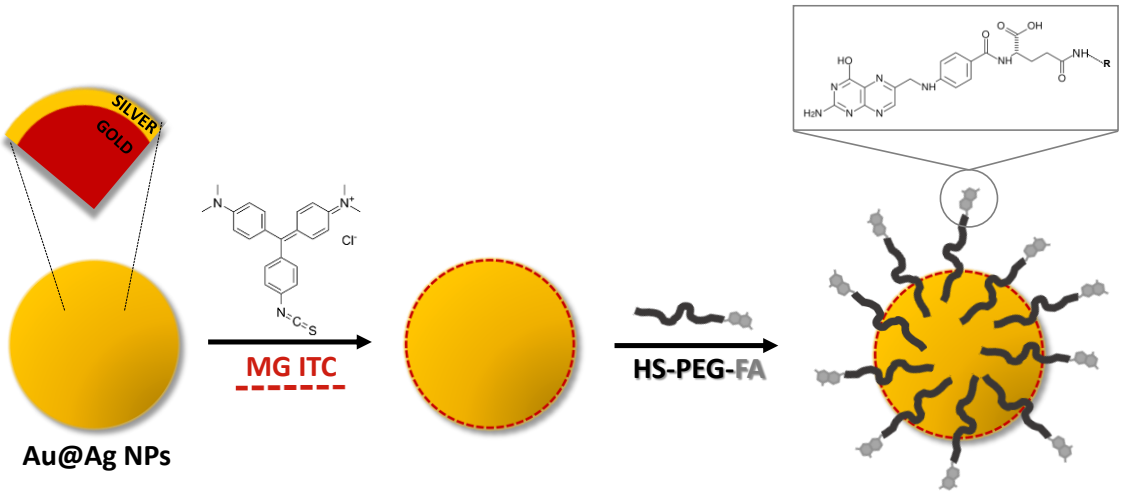

Figure 1. Schematic representation of the synthesis process of the SERS nanotags targeting Folate Receptor α.

These results were supported by dynamic light scattering and zeta potential measurements. The average hydrodynamic diameter of the bare Au@Ag NPs was 53 ± 2 nm (**Figure 2B**). The core gold NPs have an initial average diameter of 41 ± 1 nm (**Figure S3**), confirming the deposition of a silver shell of approximately 7.5 nm. The zeta potential of the bare Au@Ag NPs was -26 ± 1 mV, insuring the colloidal stability of the NPs thanks to the citrate ions present at their surface (**Figure 2D**). After functionalisation with MGITC, the average hydrodynamic diameter slightly increased to 55 ± 1 nm but this increase was not considered significant (**Figure 2B**). The zeta potential changed from -26 ± 1 mV to -23 ± 1 mV, indicating that some negatively-charged citrate molecules were displaced by the positively-charged MGITC molecule at the surface of the NPs. The change in the zeta potential was not huge due to the small amount of MGITC used for functionalisation that was required to prevent irreversible aggregation of the NPs as mentioned above. The addition of HS-PEG-FA induced a large increase in the average hydrodynamic diameter from 55 ± 1 nm to 105 ± 3 nm, which is due to the length of the linker (about 115 monomeric units) and its hydrophilic nature (**Figure 2B**). We evaluated, by UV-Vis titration, the average number of HS-PEG-FA chains immobilised per nanoparticle to be 7600 ± 800 (**Figure S4**) in our synthesis conditions. The zeta potential further increased to -17.2 ± 0.5 mV, again due to the displacement of citrate ligands (**Figure 2D**).

Nevertheless, the nanotags did not lose stability due to this as the PEG linker introduced steric hindrance efficiently stabilising them. We then evaluated the potential aggregation of the formed nanotags in complex media. When the nanotags were suspended in PBS or in DMEM cell culture media, the average hydrodynamic diameter slightly increases compared to the diameter in MilliQ water (118 ± 3 nm in PBS, 122 ± 6 nm in DMEM, **Figure 2B**). This increase is likely due to (i) a slight aggregation due to the increased complexity of these media (polydispersity index increases from 0.26 in water to 0.35 in PBS and to 0.37 in DMEM, **Figure S5**) and (ii) a possible coordination effect between the PEG linker and larger cations present in both media [52]. However, the aggregation was low and controlled as no significant changes were observed in the UV-Vis spectrum of the nanotags stored in PBS for three days (**Figure 2E**). Additionally, the average hydrodynamic diameter also remained constant for three days

(**Figure 2C**), clearly indicating that the nanotags did not suffer from any significant aggregation. In comparison, MGITC functionalised nanoparticles (without PEG) exhibited fast and irreversible aggregation when incubated in PBS (**Figure S6**).

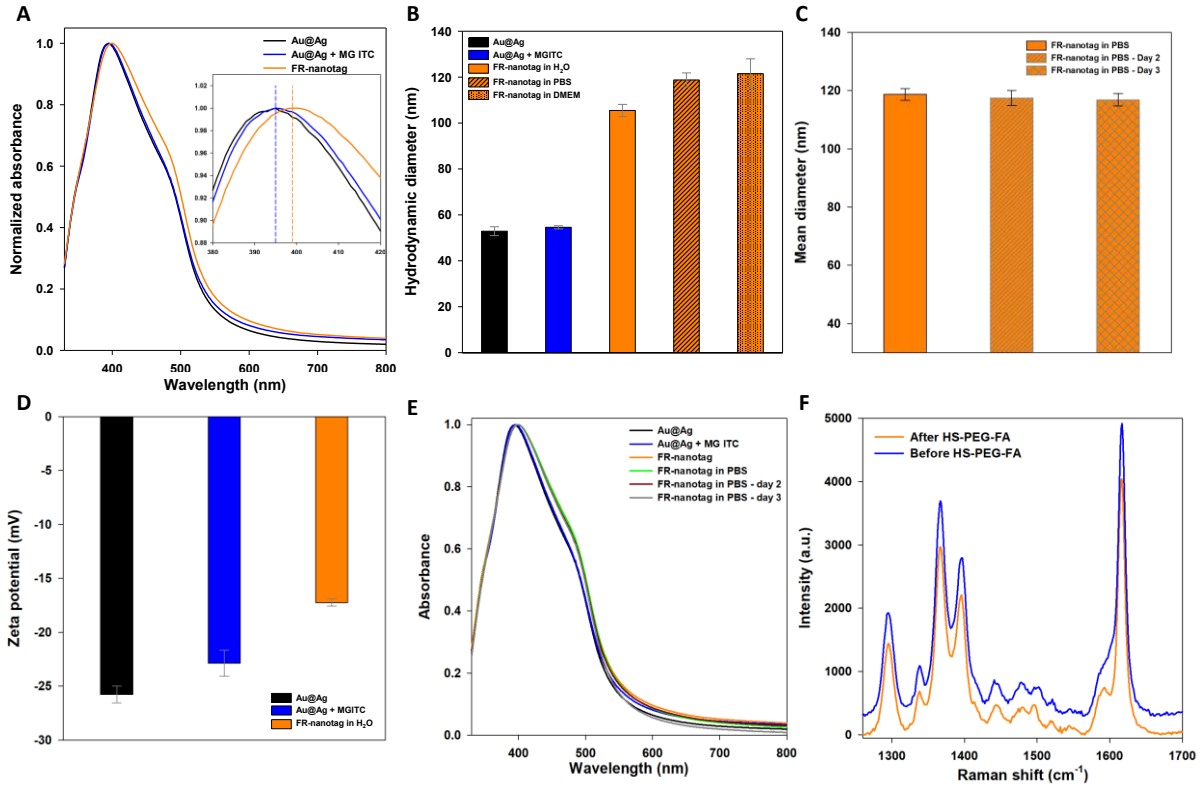

Figure 2. (A) UV-Vis spectra of the nanoparticles at different stages of the nanotag synthesis process: bare Au@Ag NPs (black), MGITC-functionalised Au@Ag NPs (blue) and HS-PEG-FA functionalised NPs (orange, final FR-nanotags). The insert shows a zoom on the region of the absorption maximum to emphasize the band red shift along the synthesis process. (B) Average hydrodynamic diameter of the NPs at different stages of the nanotag synthesis process: (i) bare Au@Ag NPs (black), (ii) MGITC-functionalised Au@Ag NPs (blue) and (iii) HS-PEG-FA functionalised NPs (final FR-nanotags) in MilliQ water (orange), in PBS buffer at pH 7.4 (dashed orange) and in DMEM cell culture media (dotted orange). (C) Evolution of the average hydrodynamic diameter of the FR-nanotags in PBS buffer over a three days period. (D) Zeta potential measured in MilliQ water (pH ≈ 3.5) of the bare Au@Ag NPs (black), MGITC-functionalised Au@Ag NPs (blue) and HS-PEG-FA functionalised NPs (orange, final FR-nanotags). (E) Evolution of the UV-Vis spectra of the FR-nanotags in PBS buffer over a three days period. (F) SERS spectra of the MGITC-functionalised NPs before (blue) and after (orange) functionalisation with HS-PEG-FA to yield the final FR-nanotags.

Finally, we characterised the SERS response of the system during the synthesis process. The bare Au@Ag NPs do not exhibit any intrinsic Raman signal under 638 nm irradiation. When MGITC was incubated with the NPs, the characteristic spectrum of this molecule appeared. The absolute SERS intensity of the MGITC signal at 1616 cm^{-1} on Au@Ag NPs is about 15 times higher than for the core gold NPs (41 ± 1 nm) and about 3 times higher than for gold nanoparticles of the same final diameter (55 ± 2 nm) (**Figure S8**). The Au@Ag NPs therefore provide an improvement in the sensitivity of detection of FRα. After functionalisation with the PEG linker, the absolute SERS intensity did not decrease significantly, indicating that the PEG linker did not remove significant amounts of MGITC molecules thanks to their strong binding to the surface through the isothiocyanate function. This is a major advantage as other popular Raman reporters that we tested were displaced by the PEG linker when tested in similar conditions, leading to loss of sensitivity (**Figure S7**). Interestingly, we observed changes in the spectrum of MGITC before and after functionalisation (**Figure 2F**). This is notably the case for the bands between 1580 and 1630 cm^{-1}, where the band at 1590 cm^{-1} is better resolved after addition of the PEG linker. These spectral changes reflect slight changes in the conformation of MGITC at the surface of the NPs due to the presence of the linker and other changes are reported in **Figure S9**. These spectral changes could be used in the future as a fast method to further confirm the successful functionalisation of the surface by the PEG linker.

Specificity of the nanotags toward Folate Receptor α

The nanotags were then evaluated to determine if they could specifically target Folate Receptor α on the surface of cancer cells. We used HeLa cells for these experiments because they exhibit a high expression of FRα [9]. To demonstrate the specificity toward FRα, we conducted experiments where the nanotags were in competition with free folic acid. We also developed a control nanotag which was coated in a PEG chain without folic acid (characterisation in **Figures S10 & S11**). Preliminary experiments determined that the optimal incubation time on HeLa cells was 4 hours (**Figure S12**) and that the viability decreased to 92 % in the presence of the 40 pM of nanotags, demonstrating that the nanotags exhibited negligible toxicity (**Figure S13**).

Control experiments were also carried out by introducing the nanotags (40 pM) in the cell culture media along with free folic acid at two concentration level (50 and 100 µM) to investigate an eventual dose-dependent behaviour. To evaluate the binding of the nanotags in the different conditions, we used Raman mapping of single cells and DCLS analysis to extract the pure spectral component of the nanotags. In each condition, we mapped several cells and evaluated the percentage of SERS-responsive pixels. A higher percentage of SERS-responsive pixels is associated with a higher binding of the nanotags to the cells, and therefore to a higher expression or availability of FRα.

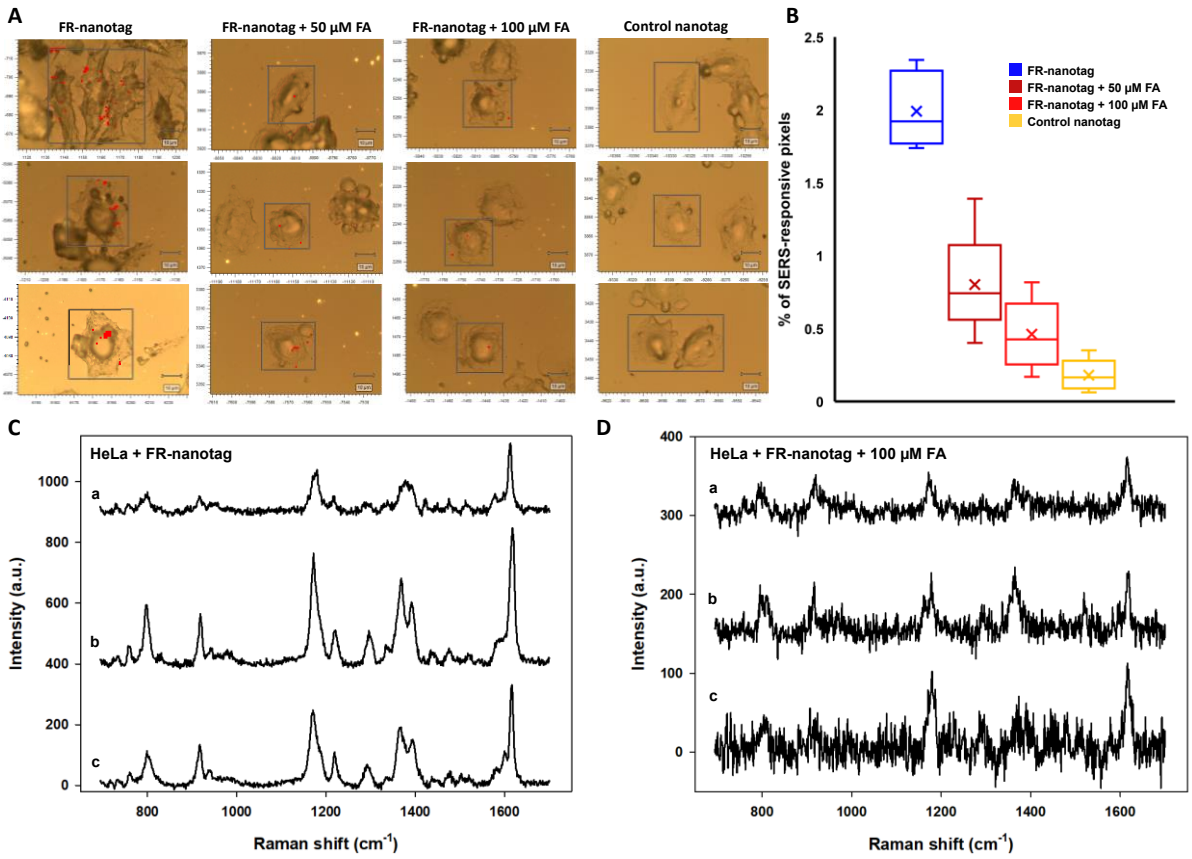

Figure 3. (A) Overlay, for some representative HeLa cells, of the SERS-active pixels highlighted by the DCLS analysis and of the cells optical images in various experimental conditions. SERS mapping was performed with a step size of 1 µm in both x and y directions, using a 50x (NA 0.75) objective and the 633 nm line of a He-Ne laser (1s of acquisition, 8 mW power at the sample). Scale bar is 10 µm. (B) Boxplot of the percentage of SERS-responsive pixels obtained in the different experimental conditions on HeLa cells. (C) Representative average SERS spectra of three HeLa cells incubated only with the FR-nanotags. (D) Representative average SERS spectra of three HeLa cells incubated with the FR-nanotags and 100 µM folic acid. Representative spectra were constructed by averaging spectra of the pixels highlighted by the DCLS analysis in each condition.

HeLa cells incubated only with the nanotags exhibit a high percentage of SERS-responsive pixels (2.0 ± 0.3 %) indicating a high binding of nanotags (**Figure 3B**). Additionally, the coefficient of variation is small (12 %), indicating that the binding is consistent among several single cells and therefore that

the level of expression of FRα is high in all mapped cells (**Figure S14**). **Figure 3C** shows, for three representative HeLa cells incubated with the nanotags, the SERS spectra obtained by averaging all the spectra highlighted by the DCLS analysis for a particular cell. We obtained in all cases a high SERS intensity for MGITC and spectra with a high signal-to-noise ratio (SNR), consistent with a high binding of the nanotags. Moreover, the spectra are similar to the reference spectrum of MGITC and do not show additional bands, indicating that the PEG coating is efficiently shielding the Raman-reporter and the silver surface from proteins in the biological media.

The percentage of SERS-responsive pixels was significantly lower on the cells incubated with the nanotags and free folic acid (0.8 ± 0.4 % for 50 µM FA, 0.5 ± 0.2 % for 100 µM FA). **Figure 3D** shows some representative SERS spectra obtained by averaging the spectra highlighted by the DCLS analysis on HeLa cells incubated with 100 µM folic acid. As can be seen, the SERS intensity for MGITC and the SNR are lower than for HeLa cells incubated only with the nanotags (**Figure 3C**). This is consistent with a lower binding of the nanotags in these conditions. Moreover, the percentage of SERS-responsive pixels is lower on the cells incubated with the highest concentration of free folic acid (100 µM), suggesting a dose-dependent effect. These results clearly demonstrate that the presence of free folic acid in the media gradually blocks folate receptors (more FRα remain available for the nanotags with 50 µM FA than with 100 µM FA), resulting in a gradually lower binding of the nanotags compared to media without any added folic acid.

Finally, we incubated the control nanotag in the same conditions (40 pM, 4 hours) and we observed almost no binding on the HeLa cells (average percentage of SERS-responsive pixels is 0.2 ± 0.1 %). The very low level of binding observed for the control nanotags demonstrates that the folic acid molecule at the end of the PEG chain is responsible for the binding of the FR-nanotags on the cells. Functionalisation with folic acid allows 10-times higher binding of nanotags to the cells. It is already well known that nanotags with no targeting moiety at the end of the PEG chain exhibits very low level of binding on cells when incubated for short period [53]. Therefore, we demonstrated that the developed nanotags are highly specific for FRα and could be used to distinguish cells with variable expression of these receptors.

Identification of Folate Receptor α overexpressing cells using SERS

The purpose of the developed nanotags is to highlight cancerous cells that overexpress FRα with the future goal of selecting more efficiently tumors that could be treated with FRα-targeted drugs. Therefore, we performed experiments on a second cancerous cell line to compare its expression of FRα to HeLa cells. A549 cells are regularly used as negative control for FRα-targeting applications as they express very low level of FRα [54]. In this experiment, we incubated the nanotags with HeLa and A549 cells in identical experimental conditions (40 pM, 4 hours incubation) and we evaluated the percentage of SERS-responsive pixels on each cell line after Raman mapping of several single cells. We observed a very large and significant difference in the percentage of SERS-responsive pixels between the two cell lines. HeLa cells exhibit high binding with the nanotags (2.0 ± 0.3 % of SERS-responsive pixels) whereas A549 cells exhibit a low level of binding with the nanotags (0.5 ± 0.1 % of SERS-responsive pixels). Representative average SERS spectra obtained for HeLa (**Figure 4C**) and A549 (**Figure 4D**) cells incubated with the nanotags only indicated a very clear difference. The SERS spectrum associated with HeLa cells exhibits higher intensity of MGITC signal and higher SNR compared to the spectrum associated with A549 cells, confirming the higher binding of nanotags on HeLa cells.

We obtain a very clear contrast between the two cell lines due to their different expression level of FRα. The percentage of SERS-active pixels is 4-fold higher on HeLa cells than on A549 cells. This is an important improvement since our previous system composed of poly(allylamine)-coated Au@Ag NPs functionalised with folic acid only achieved a 1.8-fold higher signal on FRα-overexpressing cells [49]. We believe that this improvement of contrast is due to the PEG linker that reduces unspecific interactions more efficiently than poly(allylamine).

Therefore, using the developed nanotags, we can very efficiently distinguish between FRα-overexpressing and non-overexpressing cancerous cells. We also conducted experiments on A549 cells with free folic acid (100 µM) along with the nanotags and did not observe any statistically significant difference compared to A549 incubated only with the nanotags (**Figure 4D**). Our hypothesis is that the signals detected during the Raman mapping on A549 cells were probably due to non-specific binding and not to true binding with FRα. Therefore, the additional folic acid present in the media was not able to induce any decrease in binding of the nanotags.

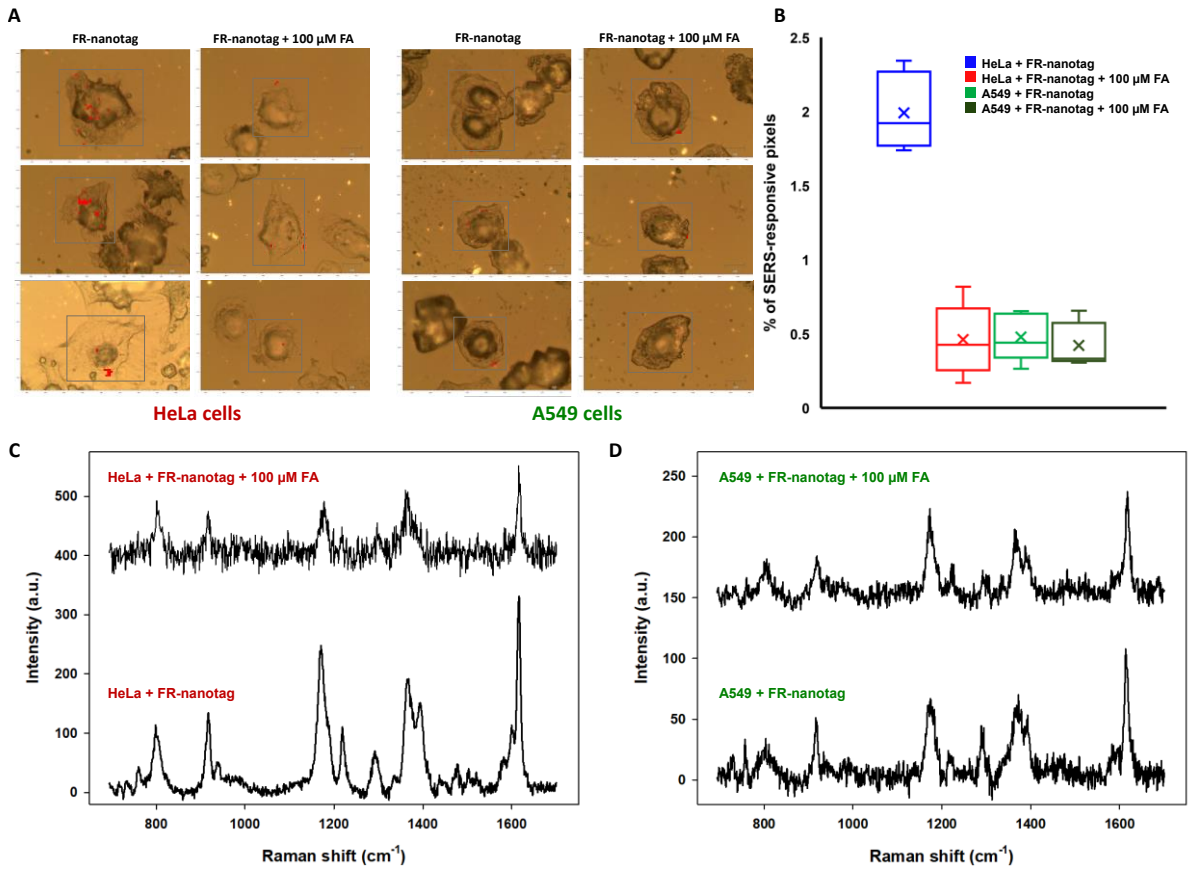

Figure 4. (A) Overlay, for some representative HeLa and A549 cells, of the SERS-active pixels highlighted by the DCLS analysis and of the cells optical images in various experimental conditions. SERS mapping was performed with a step size of 1 µm in both x and y directions, using a 50x (NA 0.75) objective and the 633 nm line of a He-Ne laser (1s of acquisition, 8 mW power at the sample). Scale bar is 10 µm. (B) Boxplot of the percentage of SERS-responsive pixels obtained on HeLa and A549 cells in the different experimental conditions. (C) Representative average SERS spectra of HeLa cells incubated only with the FR-nanotags (bottom) or with the FR-nanotags and 100 µM folic acid (top). (D) Representative average SERS spectra of A549 cells incubated only with the FR-nanotags (bottom) or with the FR-nanotags and 100 µM folic acid (top). Representative spectra were constructed by averaging spectra of the pixels highlighted by the DCLS analysis in each condition.

Interestingly, the level of SERS-active pixels reached for A549 cells (0.5 ± 0.1 %) is very similar to the level obtained for HeLa cells in the presence of 100 µM folic acid (0.5 ± 0.2 %). It indicates that 100 µM of folic acid was a sufficient concentration to block virtually all available FRα on HeLa cells, leading to a residual signal attributed mainly to non-specific binding. This is confirmed by the representative average SERS spectra obtained in the various conditions explained previously (**Figures 4C and 4D**). Spectra obtained for HeLa + nanotags + 100 µM FA, A549 + nanotags and A549 + nanotags + 100 µM FA all show similar intensity and SNR for the MGITC signal, suggesting a similar level of binding between these three conditions. Therefore, 0.5% of SERS-responsive pixels can be seen as the background threshold level of binding and any cells with higher percentages can be viewed as expressing high and detectable levels of FRα. This feature makes the developed nanotags highly effective at highlighting only cells with high levels of FRα. Finally, the background threshold of binding identified (around 0.5 % of SERS-responsive pixels) was higher than the level of binding of the control

nanotag (0.2 ± 0.1 %) (**Figure 3B**), indicating that the folic acid molecule at the end of the PEG chain on the nanotags may induce more non-specific interactions than bare PEG chains.

Folate Receptor α targeting on live cells: comparison with fixed cells

The FR-nanotags were then tested on live cells and the results compared with those obtained previously on fixed cells. The main difference comes from the absence of a formaldehyde fixing step and drying of the cells before the SERS mapping.

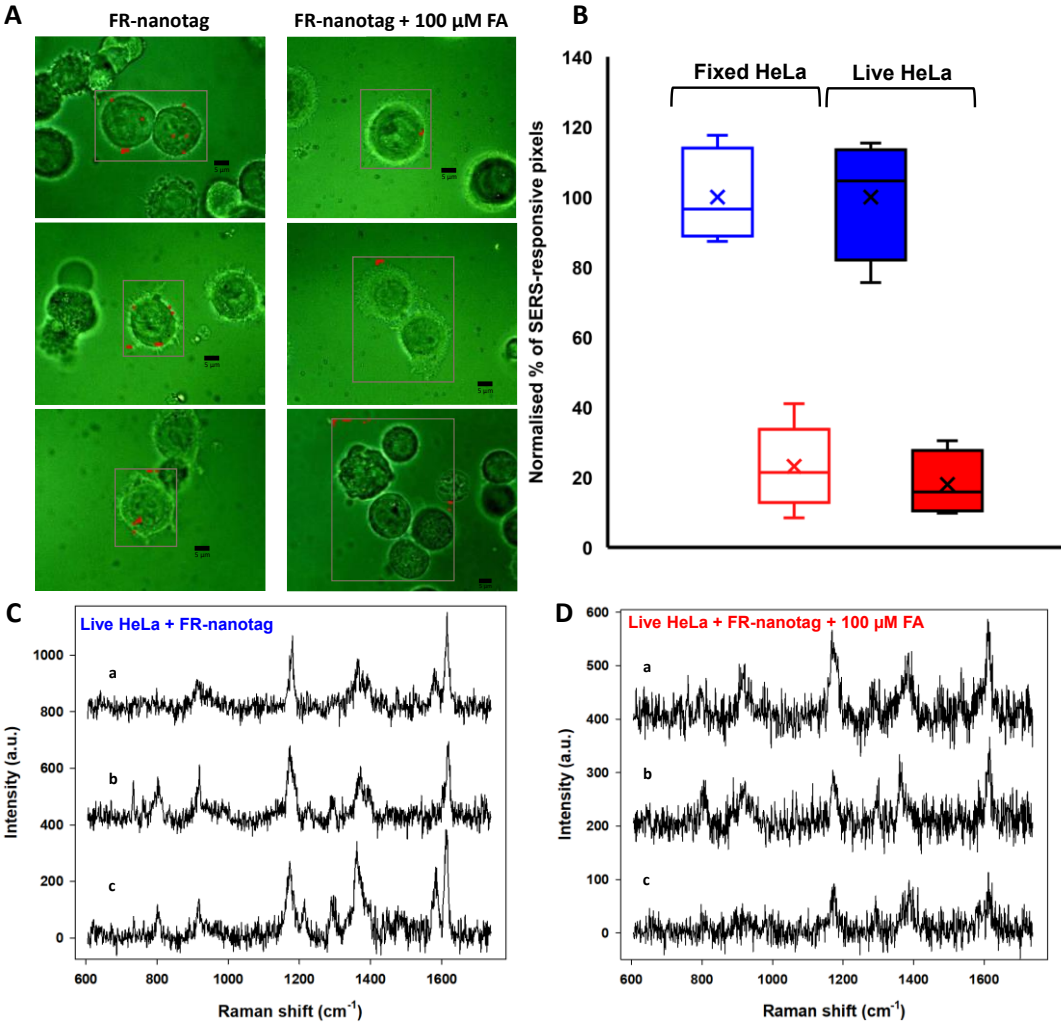

Figure 5. (A) Overlay, for some representative live HeLa cells, of the SERS-active pixels highlighted by the DCLS analysis and of the cells optical images in various experimental conditions. SERS mapping was performed with a step size of 1 µm in both x and y directions, using a 60x (NA 1.0) water immersion objective and the 633 nm line of a He-Ne laser (0.5 s of acquisition, 4 mW power at the sample). Scale bar is 5 µm. (B) Boxplot of the normalised percentage of SERS-responsive pixels obtained on live and fixed HeLa cells in the two different experimental conditions studied: FR-nanotags only (blue boxes) or FR-nanotags + 100 µM folic acid (red boxes). Percentage were arbitrarily normalised to a value of 100 for the results obtained on HeLa cells incubated only with the nanotags in both live and fixed conditions to allow proper comparison. (C) Representative average SERS spectra of three live HeLa cells incubated only with the FR-nanotags. (D) Representative average SERS spectra of three live HeLa cells incubated with the FR-nanotags and 100 µM folic acid. Representative spectra were constructed by averaging spectra of the pixels highlighted by the DCLS analysis in each condition.

These differences may influence the SERS signal due to crosslinking of proteins in the cellular membrane, or due to aggregation of the nanotags during the drying process that may create hot-spots. It is therefore interesting to compare the results provided by the nanotags when used on live cells. HeLa cells were chosen since the nanotags did not induce significant toxicity on these cells when introduced in combination with free folic acid. HeLa cells were mapped after 4 hours of incubation with (i) FR-targeted nanotags (40 pM) or (ii) FR-targeted nanotags (40 pM) with free folic acid (100 µM). **Figure 5A** shows that the number of pixels highlighted by the DCLS analysis is higher for cells incubated only

with the nanotags than for cells incubated also with folic acid. This is consistent with results from fixed cells mapping. **Figure 5C** shows representative spectra obtained from the mapping of HeLa cells in the presence of the nanotags only.

Spectra show the characteristic spectrum of MGITC but with a lower intensity and SNR than the spectra obtained on fixed cells. This is due to the slightly different acquisition parameters used during the mapping. Indeed, spectral acquisition time was reduced from 1 to 0.5 s and laser power was reduced by a factor of 2 to avoid any damage to the live cells. We also observed a slight change in the MGITC spectrum compared to the reference spectrum for one of the MGITC spectra shown (Figure 5C, spectrum (c)), which is likely due to the live cells providing an additional challenge to the PEG coating due to their dynamic nature, resulting in a potential change in the MGITC environment. Further experiments are needed to better understand the spectral changes observed.

In a similar manner than for the fixed cells, the spectra obtained on cells incubated also with folic acid show even lower signal intensity and SNR for MGITC (**Figure 5D**). This is consistent with a lower binding of the nanotags when folic acid is present in high amount in the media. To properly compare the results from fixed and live cells experiments, we computed the percentage of SERS-responsive pixels in both experimental conditions and we normalised the value obtained for HeLa cells with the nanotags (both live and fixed) to an arbitrary value of 100. By doing so, we can compare the contrast obtained when folic acid was introduced in the media. As can be seen in **Figure 5B**, the contrast between conditions with the nanotags only and with the nanotags + 100 µM folic acid is almost equivalent between fixed and live cells. These results indicate that the fixing step does not interfere with the detection of the relative amounts of nanotags bond to the cells, and by extension do not interfere with the detection of FRα-overexpressing cells. It also indicates that the developed nanotags can be readily used before cell fixation or on live cells without adaptation, which makes them a versatile tool for SERS cellular measurements.

Conclusion

In this work, we developed SERS nanotags for the detection of Folate Receptor α on single cells. We used Au@Ag core@shell nanoparticles functionalised with a resonant Raman-reporter molecule to reach a high, quantitative sensitivity of detection and a PEG-FA linker to simultaneously stabilise the nanotags and provide them with targeting properties toward FRα. We demonstrated that the functionalisation of the nanotags with a PEG linker bearing folic acid allows the highly specific targeting of FRα. The nanotags could also be applied for the monitoring of the gradual blocking of FRα. The results indicated that the HeLa cells exhibited a 10-times higher SERS response when folic acid was present on the PEG linker. Also, the level of binding of the control nanotag was lower than the binding of the FR-nanotags in the presence of excess folic acid, suggesting that the folic acid molecules on the PEG chains is responsible for a significant part of the non-specific interactions experienced by the nanotags. Using the developed nanotags, we could discriminate FRα-overexpressing from non-overexpressing cancerous cells by obtaining a 4-times higher SERS response on overexpressing HeLa cells than on non-overexpressing A549 cells. Finally, we took advantage of the low toxicity of the nanotags to compare results of SERS mapping on fixed and live HeLa cells. We showed that there was no significant difference in the detection of FRα between both experimental conditions, indicating that the developed nanotags can be readily used in both live and fixed experiments. In the future, more drugs will likely be developed to target FRα and therefore those nanotags could be used to monitor in real time the expression of FRα in response to treatment. They could also be used on patient-derived cellular

cultures, an emerging in-vitro diagnosis modality [55], to measure the potential overexpression of FRα and further guide the choice of treatment.

Acknowledgements

Sian Sloan-Dennison and Duncan Graham acknowledge financial support from the Medical Research Council (MRC) through grant number MR/V038303/1.

References

[1] S. Jeong, M.-J. Park, W. Song, and H.-S. Kim, "Current immunoassay methods and their applications to clinically used biomarkers of breast cancer," *Clin. Biochem.*, vol. 78, pp. 43–57, 2020, doi: https://doi.org/10.1016/j.clinbiochem.2020.01.009.

[2] M. Labib and S. O. Kelley, "Single-cell analysis targeting the proteome," *Nat. Rev. Chem.*, vol. 4, no. 3, pp. 143–158, 2020, doi: 10.1038/s41570-020-0162-7.

[3] Y. T. Lee, Y. J. Tan, and C. E. Oon, "Molecular targeted therapy: Treating cancer with specificity," *Eur. J. Pharmacol.*, vol. 834, no. June, pp. 188–196, 2018, doi: 10.1016/j.ejphar.2018.07.034.

[4] C. H. Chau, P. S. Steeg, and W. D. Figg, "Antibody–drug conjugates for cancer," *Lancet*, vol. 394, no. 10200, pp. 793–804, 2019, doi: 10.1016/S0140-6736(19)31774-X.

[5] C. Zhuang, X. Guan, H. Ma, H. Cong, W. Zhang, and Z. Miao, "Small molecule-drug conjugates: A novel strategy for cancer-targeted treatment," *Eur. J. Med. Chem.*, vol. 163, pp. 883–895, 2019, doi: 10.1016/j.ejmech.2018.12.035.

[6] G. Zhu, G. Niu, and X. Chen, "Aptamer-Drug Conjugates," *Bioconjug. Chem.*, vol. 26, no. 11, pp. 2186–2197, 2015, doi: 10.1021/acs.bioconjchem.5b00291.

[7] R. A. Burrell, N. McGranahan, J. Bartek, and C. Swanton, "The causes and consequences of genetic heterogeneity in cancer evolution," *Nature*, vol. 501, no. 7467, pp. 338–345, 2013, doi: 10.1038/nature12625.

[8] A. Cheung *et al.*, "Targeting folate receptor alpha for cancer treatment," *Oncotarget*, vol. 7, no. 32, pp. 52553–52574, 2016, doi: 10.18632/oncotarget.9651.

[9] K. Siwowska, R. Schmid, S. Cohrs, R. Schibli, and C. Müller, "Folate Receptor-Positive Gynecological Cancer Cells: In Vitro and In Vivo Characterization," *Pharmaceuticals*, vol. 10, no. 3, p. 72, 2017, doi: 10.3390/ph10030072.

[10] M. Scaranti, E. Cojocaru, S. Banerjee, and U. Banerji, "Exploiting the folate receptor α in oncology," *Nat. Rev. Clin. Oncol.*, vol. 17, no. 6, pp. 349–359, 2020, doi: 10.1038/s41571-020-0339-5.

[11] A. S. Wibowo *et al.*, "Structures of human folate receptors reveal biological trafficking states and diversity in folate and antifolate recognition," *Proc. Natl. Acad. Sci. U. S. A.*, vol. 110, no. 38, pp. 15180–15188, 2013, doi: 10.1073/pnas.1308827110.

[12] R. Zhao, N. Diop-Bove, M. Visentin, and I. D. Goldman, "Mechanisms of membrane transport of folates into cells and across epithelia," *Annu. Rev. Nutr.*, vol. 31, pp. 177–201, Aug. 2011, doi: 10.1146/annurev-nutr-072610-145133.

[13] S. Wang and P. S. Low, "Folate-mediated targeting of antineoplastic drugs, imaging agents, and nucleic acids to cancer cells," *J. Control. Release*, vol. 53, no. 1–3, pp. 39–48, 1998, doi: 10.1016/S0168-3659(97)00236-8.

[14] C. Chen *et al.*, "Structural basis for molecular recognition of folic acid by folate receptors," *Nature*, vol. 500, no. 7463, pp. 486–489, 2013, doi: 10.1038/nature12327.

[15] D. Feng, Y. Song, W. Shi, X. Li, and H. Ma, "Distinguishing Folate-Receptor-Positive Cells from Folate-Receptor-Negative Cells Using a Fluorescence Off–On Nanoprobe," *Anal. Chem.*, vol. 85, no. 13, pp. 6530–6535, Jul. 2013, doi: 10.1021/ac401377n.

[16] Y. Song, W. Shi, W. Chen, X. Li, and H. Ma, "Fluorescent carbon nanodots conjugated with folic acid for distinguishing folate-receptor-positive cancer cells from normal cells," *J. Mater. Chem.*, vol. 22, no. 25, pp. 12568–12573, 2012, doi: 10.1039/C2JM31582C.

[17] J. Langer *et al.*, "Present and Future of Surface-Enhanced Raman Scattering," *ACS Nano*, vol. 14, no. 1, pp. 28–

117, Jan. 2020, doi: 10.1021/acsnano.9b04224.

[18] S. S. Panikar, D. Cialla-May, E. De la Rosa, P. Salas, and J. Popp, "Towards translation of surface-enhanced Raman spectroscopy (SERS) to clinical practice: Progress and trends," *TrAC - Trends Anal. Chem.*, vol. 134, p. 116122, 2021, doi: 10.1016/j.trac.2020.116122.

[19] M. M. Joseph *et al.*, "Exploring the margins of SERS in practical domain: An emerging diagnostic modality for modern biomedical applications," *Biomaterials*, vol. 181, pp. 140–181, 2018, doi: 10.1016/j.biomaterials.2018.07.045.

[20] L. A. Lane, X. Qian, and S. Nie, "SERS Nanoparticles in Medicine: From Label-Free Detection to Spectroscopic Tagging," *Chem. Rev.*, vol. 115, no. 19, pp. 10489–10529, 2015, doi: 10.1021/acs.chemrev.5b00265.

[21] B. Shan, Y. Pu, Y. Chen, M. Liao, and M. Li, "Novel SERS labels: Rational design, functional integration and biomedical applications," *Coord. Chem. Rev.*, vol. 371, pp. 11–37, 2018, doi: 10.1016/j.ccr.2018.05.007.

[22] Y. Wang, Y. Zhang, and S. Schlücker, "Chapter 17 - Immuno-SERS: from nanotag design to assays and microscopy," Y. Ozaki, M. Baranska, I. K. Lednev, and B. R. B. T.-V. S. in P. R. Wood, Eds. Academic Press, 2020, pp. 485–528.

[23] Z. Wang, S. Zong, L. Wu, D. Zhu, and Y. Cui, "SERS-Activated Platforms for Immunoassay: Probes, Encoding Methods, and Applications," *Chem. Rev.*, vol. 117, no. 12, pp. 7910–7963, 2017, doi: 10.1021/acs.chemrev.7b00027.

[24] B. Lutz *et al.*, "Raman nanoparticle probes for antibody-based protein detection in tissues," *J. Histochem. Cytochem.*, vol. 56, no. 4, pp. 371–379, 2008, doi: 10.1369/jhc.7A7313.2007.

[25] A. Verdin, C. Malherbe, and G. Eppe, "Spatially resolved determination of the abundance of the HER2 marker in microscopic breast tumors using targeted SERS imaging," *Microchim. Acta*, vol. 188, no. 9, pp. 10–12, 2021, doi: 10.1007/s00604-021-04943-6.

[26] M. Bhamidipati, H. Y. Cho, K. B. Lee, and L. Fabris, "SERS-Based Quantification of Biomarker Expression at the Single Cell Level Enabled by Gold Nanostars and Truncated Aptamers," *Bioconjug. Chem.*, vol. 29, no. 9, pp. 2970–2981, 2018, doi: 10.1021/acs.bioconjchem.8b00397.

[27] E. Wiercigroch *et al.*, "ImmunoSERS microscopy for the detection of smooth muscle cells in atherosclerotic plaques," *Biosens. Bioelectron.*, vol. 133, no. March, pp. 79–85, 2019, doi: 10.1016/j.bios.2019.02.068.

[28] M. Salehi, L. Schneider, P. Ströbel, A. Marx, J. Packeisen, and S. Schlücker, "Two-color SERS microscopy for protein co-localization in prostate tissue with primary antibody–protein A/G–gold nanocluster conjugates," *Nanoscale*, vol. 6, no. 4, pp. 2361–2367, 2014, doi: 10.1039/C3NR05890E.

[29] E. Stepula *et al.*, "6-Color/1-Target Immuno-SERS Microscopy on the Same Single Cancer Cell," *ACS Appl. Mater. Interfaces*, vol. 12, no. 29, pp. 32321–32327, Jul. 2020, doi: 10.1021/acsami.0c07269.

[30] X.-P. Wang, B. Walkenfort, M. König, L. König, S. Kasimir-Bauer, and S. Schlücker, "Fast and reproducible iSERS microscopy of single HER2-positive breast cancer cells using gold nanostars as SERS nanotags," *Faraday Discuss.*, vol. 205, no. 0, pp. 377–386, 2017, doi: 10.1039/C7FD00135E.

[31] Y. Zhang, X. P. Wang, S. Perner, A. Bankfalvi, and S. Schlücker, "Effect of Antigen Retrieval Methods on Nonspecific Binding of Antibody-Metal Nanoparticle Conjugates on Formalin-Fixed Paraffin-Embedded Tissue," *Anal. Chem.*, vol. 90, no. 1, pp. 760–768, 2018, doi: 10.1021/acs.analchem.7b03144.

[32] X.-P. Wang *et al.*, "iSERS microscopy guided by wide field immunofluorescence: analysis of HER2 expression on normal and breast cancer FFPE tissue sections," *Analyst*, vol. 141, no. 17, pp. 5113–5119, 2016, doi: 10.1039/C6AN00927A.

[33] K. K. Maiti, A. Samanta, M. Vendrell, K. S. Soh, M. Olivo, and Y. T. Chang, "Multiplex cancer cell detection by SERS nanotags with cyanine and triphenylmethine Raman reporters," *Chem. Commun.*, vol. 47, no. 12, pp. 3514–3516, 2011, doi: 10.1039/c0cc05265e.

[34] L. Li, M. Liao, Y. Chen, B. Shan, and M. Li, "Surface-enhanced Raman spectroscopy (SERS) nanoprobes for ratiometric detection of cancer cells," *J. Mater. Chem. B*, vol. 7, no. 5, pp. 815–822, 2019, doi: 10.1039/c8tb02828a.

[35] E. Stepula *et al.*, "Localization of PD-L1 on single cancer cells by iSERS microscopy with Au/Au core/satellite nanoparticles," *J. Biophotonics*, vol. 13, no. 3, pp. 1–7, 2020, doi: 10.1002/jbio.201960034.

[36] E. Feng, T. Zheng, X. He, J. Chen, and Y. Tian, "A novel ternary heterostructure with dramatic SERS activity for evaluation of PD-L1 expression at the single-cell level," no. JUNE, 2019.

[37] C. Hu *et al.*, "Highly narrow nanogap-containing Au@Au core–shell SERS nanoparticles: size-dependent Raman enhancement and applications in cancer cell imaging," *Nanoscale*, vol. 8, no. 4, pp. 2090–2096, 2016, doi: 10.1039/C5NR06919J.

[38] L. Guerrini, N. Pazos-Perez, E. Garcia-Rico, and R. Alvarez-Puebla, "Cancer characterization and diagnosis with SERS-encoded particles," *Cancer Nanotechnol.*, vol. 8, no. 1, p. 5, 2017, doi: 10.1186/s12645-017-0031-3.

[39] A. Kapara, V. G. Brunton, D. Graham, and K. Faulds, "Characterisation of estrogen receptor alpha (ERα) expression in breast cancer cells and effect of drug treatment using targeted nanoparticles and SERS," *Analyst*, vol. 145, no. 22, pp. 7225–7233, 2020, doi: 10.1039/d0an01532f.

[40] A. Kapara, K. A. Findlay Paterson, V. G. Brunton, D. Graham, M. Zagnoni, and K. Faulds, "Detection of Estrogen Receptor Alpha and Assessment of Fulvestrant Activity in MCF-7 Tumor Spheroids Using Microfluidics and SERS," *Anal. Chem.*, vol. 93, no. 14, pp. 5862–5871, 2021, doi: 10.1021/acs.analchem.1c00188.

[41] X. Qu, G. Qi, D. Sun, J. Yue, W. Xu, and S. Xu, "Metformin hydrochloride action on cell membrane N-cadherin expression and cell nucleus revealed by SERS nanoprobes," *Talanta*, vol. 232, no. April, p. 122442, 2021, doi: 10.1016/j.talanta.2021.122442.

[42] S. Boca-Farcau, M. Potara, T. Simon, A. Juhem, P. Baldeck, and S. Astilean, "Folic acid-conjugated, SERS-labeled silver nanotriangles for multimodal detection and targeted photothermal treatment on human ovarian cancer cells," *Mol. Pharm.*, vol. 11, no. 2, pp. 391–399, 2014, doi: 10.1021/mp400300m.

[43] Y. Chen *et al.*, "Combined Labelled and Label-free SERS Probes for Triplex Three-dimensional Cellular Imaging," *Sci. Rep.*, vol. 6, no. January, pp. 1–12, 2016, doi: 10.1038/srep19173.

[44] Z. Liu, Z. Guo, H. Zhong, X. Qin, M. Wan, and B. Yang, "Graphene oxide based surface-enhanced Raman scattering probes for cancer cell imaging," *Phys. Chem. Chem. Phys.*, vol. 15, no. 8, pp. 2961–2966, 2013, doi: 10.1039/c2cp43715e.

[45] J. Chang, A. Zhang, Z. Huang, Y. Chen, Q. Zhang, and D. Cui, "Monodisperse Au@Ag core-shell nanoprobes with ultrasensitive SERS-activity for rapid identification and Raman imaging of living cancer cells," *Talanta*, vol. 198, pp. 45–54, 2019, doi: https://doi.org/10.1016/j.talanta.2019.01.085.

[46] C. Fasolato *et al.*, "Folate-based single cell screening using surface enhanced Raman microimaging," *Nanoscale*, vol. 8, no. 39, pp. 17304–17313, 2016, doi: 10.1039/c6nr05057c.

[47] A. N. Ramya, M. M. Joseph, S. Maniganda, V. Karunakaran, S. T. T., and K. K. Maiti, "Emergence of Gold-Mesoporous Silica Hybrid Nanotheranostics: Dox-Encoded, Folate Targeted Chemotherapy with Modulation of SERS Fingerprinting for Apoptosis Toward Tumor Eradication," *Small*, vol. 13, no. 31, p. 1700819, Aug. 2017, doi: https://doi.org/10.1002/smll.201700819.

[48] Z. Zhai *et al.*, "Uptake of silver nanoparticles by DHA-treated cancer cells examined by surface-enhanced Raman spectroscopy in a microfluidic chip," *Lab Chip*, vol. 17, no. 7, pp. 1306–1313, 2017, doi: 10.1039/C7LC00053G.

[49] A. Verdin, C. Malherbe, W. H. Müller, V. Bertrand, and G. Eppe, "Multiplex micro-SERS imaging of cancer-related markers in cells and tissues using poly(allylamine)-coated Au@Ag nanoprobes," *Anal. Bioanal. Chem.*, 2020, doi: 10.1007/s00216-020-02927-8.

[50] S. Zong, Z. Wang, J. Yang, C. Wang, S. Xu, and Y. Cui, "A SERS and fluorescence dual mode cancer cell targeting probe based on silica coated Au@Ag core–shell nanorods," *Talanta*, vol. 97, pp. 368–375, 2012, doi: https://doi.org/10.1016/j.talanta.2012.04.047.

[51] W. E. Smith, "Practical understanding and use of surface enhanced Raman scattering/surface enhanced resonance Raman scattering in chemical and biological analysis," *Chem. Soc. Rev.*, vol. 37, no. 5, pp. 955–964, 2008, doi: 10.1039/B708841H.

[52] J. E. Lu and S. Chen, "Organized assembling of poly(ethylene glycol)-functionalized Janus nanoparticles induced by select alkali metal ions," *Inorg. Chem. Commun.*, vol. 110, no. October, p. 107586, 2019, doi: 10.1016/j.inoche.2019.107586.

[53] D. B. Chithrani, "Polyethylene Glycol Density and Length Affects Nanoparticle Uptake by Cancer Cells," *J. Nanomedicine Res.*, vol. 1, no. 1, pp. 1–6, 2014, doi: 10.15406/jnmr.2014.01.00006.

[54] D. Ren, F. Kratz, and S.-W. Wang, "Engineered drug-protein nanoparticle complexes for folate receptor targeting,"

Biochem. Eng. J., vol. 89, pp. 33–41, 2014, doi: 10.1016/j.bej.2013.09.008.Engineered.

[55] D. P. Kodack *et al.*, “Primary Patient-Derived Cancer Cells and Their Potential for Personalized Cancer Patient Care,” *Cell Rep.*, vol. 21, no. 11, pp. 3298–3309, 2017, doi: 10.1016/j.celrep.2017.11.051.